IEEE Open Journal of
Industry Applications

Received 2 January 2020; revised 21 February 2020; accepted 9 March 2020. Date of publication 17 March 2020;
date of current version 23 April 2020. The review of this article was arranged by Editor C. Boccaletti.

*Digital Object Identifier 10.1109/OJIA.2020.2981455*

# Interaction of Transmission-Distribution System in the Presence of DER Units–Co-simulation Approach

**MOHAMMAD MEHDI REZVANI [1] (Student Member, IEEE), SHAHAB MEHRAEEN [1] (Member, IEEE), JAYANTH R. RAMAMURTHY [2] (Senior Member, IEEE), AND THOMAS FIELD [2] (Senior Member, IEEE)**

[1] School of Electrical Engineering and Computer Science, Louisiana State University, Baton Rouge, LA 70803 USA
[2] Entergy Corporation, Jackson, MS 39213 USA

CORRESPONDING AUTHORS: MOHAMMAD MEHDI REZVANI; SHAHAB MEHRAEEN (e-mail: mrezva2@lsu.edu; smehraeen@lsu.edu)

**ABSTRACT** The effects of distribution-connected solar farms on the transmission and distribution systems are studied in this paper using a practical power system network. Both the transmission and distribution networks are modeled and co-simulated for intermittent effects of solar power and changing load profiles. These effects include flicker in both the transmission and the distribution systems, operation of the substation Load Tap Changer (LTC) and feeder regulators, and distribution feeder voltage profiles. The results of the study show a potential hunting effect causing excessive LTC operation especially during periods of high reverse power flow condition and a significant visible flicker in the distribution system but lower levels of flicker at the transmission level. It is shown that the hunting behavior of the LTC can be mitigated and downstream feeder voltage profiles can be improved via enhanced bandwidth, block operation mode, and adjusting time delay of the substation LTC controller. In addition, the inverter Volt-Var control can be used to effectively diminish excessive LTC operation based on IEEE Std 1547-2018 Volt-Var characteristics with modified settings. Finally, an enhanced load-flow algorithm with modified Jacobian is presented that incorporates the Distributed Energy Resource (DER) Volt-Var characteristics in the conventional Newton-Raphson method.

**INDEX TERMS** Distributed Energy Resource (DER), Flicker, Load Tap Changer (LTC), Volt-Var control.

## I. INTRODUCTION

Modern power systems take advantage of Distributed Energy Resources (DERs) and utilize renewable energy. Renewable power generation units that are connected at the distribution level fall under the category of DER. DERs, especially those based on Photovoltaics (PV), have attracted a lot of attention during the past decade due to potential energy savings for the customers and reduced environmental footprint [1], [2]. DERs can also be used to alleviate the feeder loading to allow increased load transfer capability. However, high penetration of DERs in the distribution grid can present challenges to the power system operation such as voltage and protection issues, fault detection, and during system restoration [3], [4].

The conventional distribution grid has been designed assuming that the electric power is carried unidirectionally from HV/MV substations downstream toward customers. As a result, the introduction of DERs on the distribution side will affect existing protection and control philosophies, and thus, overall, the distribution system's reliability could be affected [5]–[8]. The adverse effects of the DERs depend on various factors, such as feeder topology, size of the DER units, operation and control strategies, and the DER location in the network [9]–[11]. In addition to the effects on the distribution circuits, distribution-connected DER units may have an impact on the transmission voltage. Thus, tools must be developed to identify and mitigate these potential effects on transmission systems.

Supporting the power grid by the use of electrical energy storage converter-fed devices during high penetration of DERs is addressed in [12]. The injected/absorbed active/reactive power of the electrical energy storage devices is controlled by the frequency-voltage deviation of the

distribution grid. DER Reactive power control has been investigated in a number of operating modes including constant power factor, Volt-Var, active-reactive power, and constant Var modes [13]–[16]. Reactive power control of DER for high PV penetration in the distribution grid is discussed in [17]. Droop characteristics of the ac-dc converters of energy storage or DER, i.e., *P-f* and *Q-V*, to maintain the distribution grid under normal condition is also utilized in [18]. Harmonic compensation, reactive power control, voltage, and frequency support methods for the distribution grid are discussed in [19] for the distribution network. Recently, the simultaneous operation of the distribution voltage regulators and the DER reactive power control have been studied in [20]–[27]. These studies show the effectiveness of reactive power support in maintaining the distribution voltage and reduction of downstream feeder voltage regulator operations under intermittent solar power penetration.

While recent studies consider the impact of DERs on the distribution system, the substation is always assumed to be an infinite bus. In other words, the transmission system modeling is ignored and assumed to be a stiff system with infinite short circuit capacity. At higher levels of DER penetrations, the effect of the intermittent DER power on the transmission substation voltage cannot be ignored. In order to study the effect of DER penetration on the substation equipment and transmission side, the two circuits must be modeled and co-simulated together. In addition, the substation Load Tap Changer (LTC) controller characteristics can be altered in the legacy and modern devices to mitigate the excessive operations; however, this has not been adequately investigated in the existing literature.

This work utilizes a co-simulation environment that simulates the transmission network under the effect of distribution lumped load time series and intermittent output of the community solar farm connected at the distribution side. Thus, the effects of distribution DER units on the transmission network as well as the operation of the substation LTC can be observed. The LTC is modeled through a variable-turns-ratio transformer with constant and inverse time delays and variable voltage bandwidth capabilities [28]. Next, the reactive power control of the DER unit is implemented in the transmission load flow by adhering to the Volt-Var characteristics of the DER unit according to the IEEE Std 1547-2018 [15]. Various changes in the Volt-Var characteristics are considered and voltage stability is studied. By incorporating Volt-Var characteristic in the transmission jacobian matrix, load flow convergence is achieved rapidly when a tap operation is performed. Here, Volt-Var control is adopted via load flow that improves the simulation speed through larger time steps (seconds and larger) and avoids lengthy dynamic simulations of feedback controllers that typically require time steps in the range of milliseconds.

It is observed that under high penetration of DER power, excessive operation of the substation LTC is likely, especially under high reverse power flow. The LTC secondary voltage is utilized to solve the distribution load flow at each time step where line voltage regulators and switched capacitor banks are used to improve downstream voltages. It is also observed that through appropriate modification in the Volt-Var characteristic constants, a significant reduction in the LTC operation is achievable under highly intermittent DER power while the conventional or default settings may not be as effective. Limitations of the Volt-Var characteristic are also observed where excessive changes in the conventional settings could potentially lead to voltage instability. Additionally, it is noted that increasing the LTC measurement bandwidth, adoption of block operation mode, and time delay can help reduce its excessive operations under intermittent solar power. More details on the substation LTC are provided in [28]. Finally, the 10-minute flicker is calculated for the transmission and distribution voltages based on IEEE Std 1453-2015 [29]. It is observed that under the excessive operation of LTC caused by intermittent solar power, the distribution flicker is in the visible range whereas the transmission system is not affected as much.

Section II of the paper elaborates on system modeling. Section III provides simulation results and test cases. Finally, concluding remarks are provided in Section IV.

## II. NETWORK MODELING

For the purpose of this study a practical power system network served by 115 kV transmission lines in Central Arkansas is chosen, as shown in Fig. 1. The rest of the 115 kV power system network was equivalenced based on Thevenin short-circuit reduction, which is represented by two voltage-behind-Thevenin impedance sources at Station_1 and Station_BE, including the transfer impedance. Note that the substation BE is considered as a PQ bus to reflect voltage variations due to the Thevenin impedance. The 115/13.8 kV substation under study is called Station_CA, as shown in Fig. 2. Two solar farms with different capacities; namely, a 5 MW and a 20 MW (rated power of a substation transformer), are considered and connected at the downstream of the substation transformer as shown in Fig. 2. The distribution circuit has three feeders, C-101, C-102, C-104, comprising single-phase, two-phase, and three-phase combination of residential and commercial loads. The substation LTC is located upstream of the solar farms in the substation and a number of feeder line regulators are connected downstream on each distribution feeder. Lumped loads are considered at all other transmission buses. Time series of load data at 1 sample/min resolution was used for substations 1, 2, 3, 4, H, D, and BE, as well as temporal load variations at substation CA. Detailed models of feeders C102 and C104 along with an aggregate load representing feeder C101 was utilized with 1 sample/min load data obtained from SCADA.

Capacitor banks at substations 4 and CA have capacities of 20.4 MVAR and 22.5 MVAR, respectively. An LTC is used at substation CA. This load tap changer has 32 steps and a default bandwidth of 2 volts with a 115-volt center tap that corresponds to 13.8 kV, the substation transformer low-side voltage. Feeder C102 has 841 load sections and feeder C104 has 962 load sections.

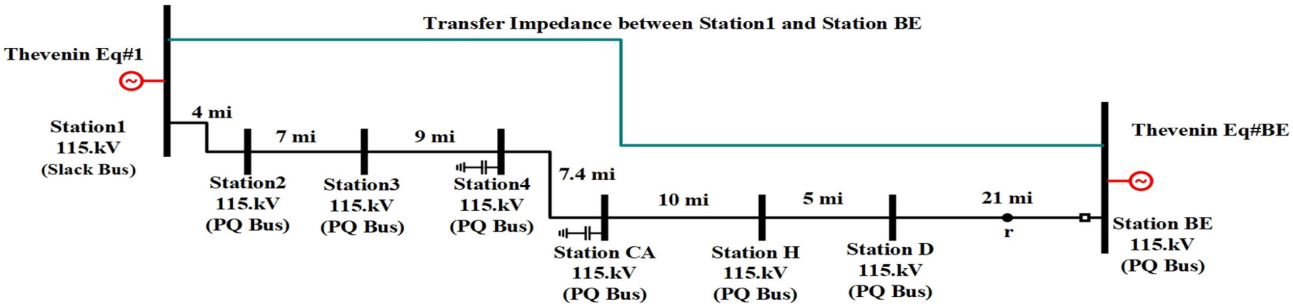


**FIGURE 1.** Multi-port Thevenin short-circuit reduced equivalent of the 115 kV transmission system.

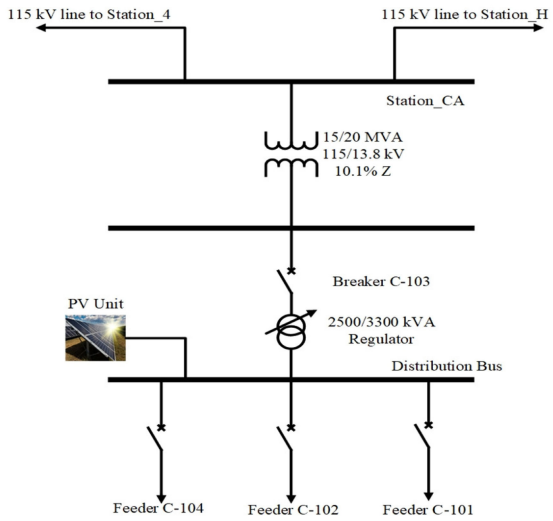


**FIGURE 2.** Substation CA along with 13.8 kV feeder.

There are three 600 kVAr capacitor banks (200 kVar/phase), one single-phase line voltage regulator and one spot load on feeder C104. Feeder C102 has four capacitor banks including two 600 kVar, a 1200 kVar, and a 300 kVar capacitor, all split equally among the three phases, along with three single-phase line voltage regulators. This information is summarized in Table 1.

### A. TIME-SERIES OF THE SOLAR GENERATION

A high-resolution time-series (1 sample/4 sec) solar power was acquired from a 140-W rooftop solar panel installed on the roof of the Renewable Energy and Smart Grid Laboratory at LSU (Latitude: 30.41, Longitude: −91.18). This high-resolution measurement provides a granular pattern of the solar generation for each day of the year. Since the network load data was only available at a resolution of 1 sample/minute, it was linearly interpolated to 4-second intervals to be consistent with the time-series of the solar data. The recorded data was then normalized for the solar farms under study. The measured load time series on a specific day from 6:00 am to 8:00 pm was merged with recorded solar production on that day for this study. The solar panels across the farm are assumed to be close enough so that the measured solar sun irradiance can be

**TABLE 1.** Summary of Network Equipment

| Transmission | | |
|---|---|---|
| | Capacitor Bank | Voltage Regulator |
| Number | 2 | 1 |
| Location | Substation 4 _ 20.4 MVAR | Substation CA |
| | Substation CA _ 22.5 MVAR | |
| **Distribution** | | |
| Capacitor Bank | Voltage Regulator | Spot load |
| 7 | 4 | 1 |
| Three on C104, 600 kVAr each | One single- phase on C104 | One on C104 |
| Four on C102 (two 600 kVAr, one 300 kVAr, and one 1200 kVAr) | Three single-phase on C102 | None on C102 |

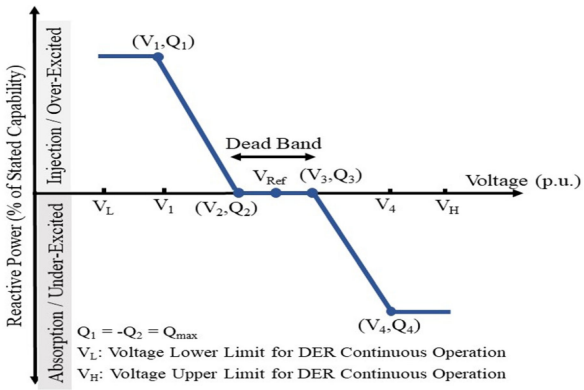


**FIGURE 3.** DER Volt/Var control method [9].

applied to all of them simultaneously. By contrast, in the case of rooftop solar panels, the footprint spans several miles and some randomness will occur in the total power generation.

### B. PV REACTIVE POWER CONTROL

The Volt-Var control is utilized at the DER unit (PV farm) to help maintain the distribution voltage. With this function, the DER unit can utilize reactive power in response to the local voltage changes. The Volt-Var curve shown in Fig. 3 is recommended by the IEEE Std 1547-2018 [15] with the

**TABLE 2. Volt-Var Control Characteristics Permittable Range [9]**

| Characteristic Voltage | Range lower - upper (p.u.) |
|---|---|
| $V_{Ref}$ | 0.95 - 1.05 |
| $V_1$ | ($V_{Ref}$ - 0.18) - ($V_2$ - 0.02) |
| $V_2$ | ($V_{Ref}$ - 0.03) - $V_{Ref}$ |
| $V_3$ | $V_{Ref}$ - ($V_{Ref}$ + 0.03) |
| $V_4$ | ($V_3$ + 0.02) - ($V_{Ref}$ + 0.18) |
| $Q_1$ and $Q_2$ | 0.44*$S_{rated}$ |

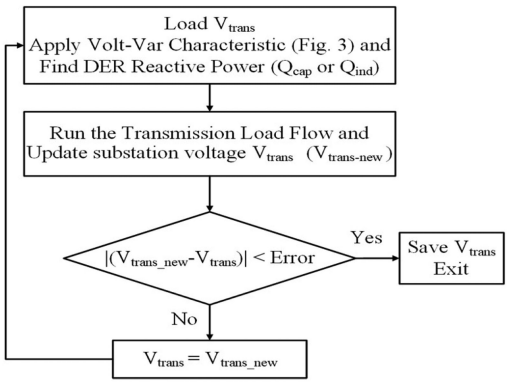


**FIGURE 4. Error Loop for Volt-Var Control.**

constants ($V_1$ through $V_4$) shown in Table 2 as recommended by the Standard. These values, however, can be altered based on the allowable range in the Standard. This work studies alterations to these constants to achieve stable Q-control that mitigates the excessive tap operations.

The injected/absorbed reactive power by the DER unit is calculated using:

$$Q_{cap} = \frac{-Q_{\max}}{V_2 - V_1} * (V - V_1) + Q_{\max} \tag{1}$$

$$Q_{inj} = \frac{Q_{\min}}{V_4 - V_3} * (V - V_3) \tag{2}$$

Due to frequent changes in the solar power (every 4 s) load flow must be conducted frequently; i.e., at every sampling time.

Since the DER unit is connected to the transmission substation, it is essentially a generation unit in the transmission system. In order to implement the Volt-Var characteristic into the load flow simulation, first, an error loop is created where the substation voltage is applied to the Volt-Var characteristic and the resultant reactive power is fed back to the Newton-Raphson transmission load flow. If the new voltage is close to the previously used one, the loop is stopped. Otherwise, once again the substation voltage from load flow is used to obtain Q from the Volt-Var characteristic. This process is shown in Fig. 4.

*Remark 1:* Our observations indicate that convergence of the loop highly depends on the slope of the characteristic in the capacitive and/or inductive regions of the Volt-Var characteristic and not too much on the dead-band (i.e., the region between $V_2$ and $V_3$). Once the slope exceeds certain levels, the error loop does not converge. Table 5 in the Simulation section compares different Volt-Var characteristics and their effects on the load flow convergence as well as the number of LTC operations.

*Remark 2:* With an appropriate Volt-Var characteristic, the error loop typically converges in just a few iterations (one iteration for Error $= 10^{-5}$, see Fig. 4). However, upon a discrete change in the network, such as tap operation, a large number of iterations are needed for convergence. Thus, a modification in the load flow is utilized such that the Volt-Var characteristic is directly implemented in the load flow jacobian matrix.

The Volt-Var characteristic is rebuilt using equations (1) and (2), and derivatives with respect to voltage are added to the jacobian matrix for the transmission load flow. Specifically, the reactive power term for the substation node is modified to (3).

$$0 = -\sum_{k=1}^{N} |V_i|\,|V_k|\,|Y_{ik}|\ \sin(\theta_i - \theta_k + \varphi_{ik}) - Q_{DER} \tag{3}$$

where $i$ and $N$ represent substation node and the total number of transmission nodes, respectively. $Q_{DER}$ can be obtained by (4).

$$Q_{DER} = \begin{cases} Q_{\max} & \text{for } V < V_1 \\ Q_{cap} = \frac{-Q_{\max}}{V_2 - V_1} * (V - V_1) + Q_{\max} & \text{for } V_1 \le V \le V_2 \\ 0 & \text{for } V_2 \le V \le V_3 \\ Q_{ind} = \frac{Q_{\min}}{V_4 - V_3} * (V - V_3) & \text{for } V_3 \le V \le V_4 \\ -Q_{\max} & \text{for } V_4 \le V \end{cases}, \tag{4}$$

and $Q_{\max}$ is the magnitude of maximum absorbed reactive power ($Q_{\min} = -Q_{\max}$). When calculating $\frac{\partial Q}{\partial V}$ at the transmission substation node, the same conditions in (4) apply. A potential problem with the $\frac{\partial Q}{\partial V}$ involving conditions in (4) is the abrupt changes in the derivatives at the Volt-Var curve break points; i.e., at points $V_1$, $V_2$, $V_3$, and $V_4$ that could potentially cause the Newton-Raphson algorithm to converge in a large number of iterations or not converge at all. Thus, the results of the two load flows are compared over the load and solar variations in the entire day as shown in Fig. 14 of Section III.B. The results of the two methods (error loop and jacobian matrix) match very well while the latter is 10–15 times faster in convergence upon discrete changes due to tap operations. These simulation results indicate the suitability of the modified jacobian.

### C. SUBSTATION VOLTAGE REGULATOR

The substation voltage regulator controls the action of the LTC of the substation transformer. The LTC measurement transformer reduces the distribution voltage of 13.8 kV to 115 V as a default bandcenter. The bandcenter can be adjusted

from 100 V to 135 V in 0.1 V increment. The bandwidth of this voltage regulator is 2 volts per step around the 115-volt bandcenter; however, it can be increased or decreased by 0.1 V increment until it reaches to 10 V or 1 V as upper and lower limits, respectively. The LTC has 32 steps, 16 steps for increasing and 16 steps for decreasing the voltage at the distribution bus. There is a time delay between each two consecutive tap operations due to the mechanical motion of the LTC (default 4 s) and another adjustable time delay after issuing a command (default 30 s). The latter is adjustable from 1 second to 120 seconds in 1-second increment. Moreover, this time delay can be definite, which means the time delay is constant at all times, or inverse, which means time delay changes based on the voltage deviation in an inverse fashion. The operating mode of the LTC during the reverse power flow is selected from the following modes: Ignore (the control will act as the forward direction), Block (it prevents automatic tap change operation); and Return to Neutral (tap position is driven to the neutral). Here, ignore and block are considered as two different control modes of LTC during reverse power flow in the simulation section.

The voltage regulator observes the voltage downstream of the substation transformer and each time the measured voltage exceeds the bandwidth, for the 2-volt band; i.e., 114 V or 116 V, it moves the tap to an upper or lower position, respectively, and thus, each tap operation results in $\frac{bandwidth}{bandcenter} \times V_{base_{dist}}$ voltage (here $\frac{2}{115} \times 13800 = 240\ V$) increase/decrease at the distribution line. The voltage regulator checks the distribution voltage based on the Time Delay setting (every 30 seconds for example) and if the voltage is outside the permissible range, it operates the LTC after the set time delay to avoid chattering of the mechanical parts. Adjustments to bandwidth and time delay are available and create more flexibility in the newer LTC mechanisms.

*Remark 3:* In most applications, an LTC bandwidth of 2 V is preferred and recommended by the manufacturers. It is also noted that each tap alters the voltage by ratio 2/115 of the base voltage. For the LTC bandwidth of 2 V, the amount of voltage change is equal to the bandwidth. That is if the voltage on the measurement transformer drops slightly below 114 V (the lower voltage limit) the LTC operates one tap and the voltage is increased by 2/115 of the 115 V bandcenter which is equal to 2 V, and thus reaches the upper limit of 116V. Under normal operation, an increase in the voltage reduces the losses due to the current drop when constant loads exist, and thus voltage is likely to further increase and cross the upper limit (116V). This initiates a reduction in the tap; i.e., chattering or hunting effect. In the real system, however, loads are combinations of constant loads, impedance loads, constant current, etc., and thus, the chance of hunting action is low.

*Remark 4:* In the event that inverter-based power generation such as solar exists at high penetration levels, the net load may look more like a constant-power load due to the power control mechanism at the DERs. In such events, the hunting action is likely and is verified by our simulation results. A number of solutions are proposed here to remedy the excessive operation of the LTC.

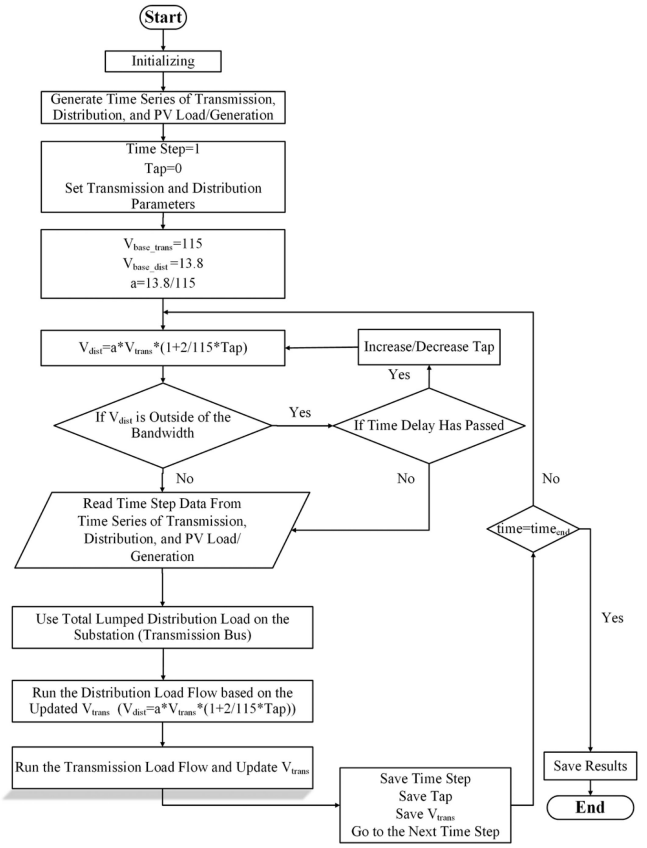


**FIGURE 5.** Universal Distribution + Transmission Load Flow Flowchart.

### D. DISTRIBUTION LOAD FLOW

Load flow is performed by employing the EPRI OpenDSS simulator [30] at the distribution level once the transmission load flow (Newton-Raphson algorithm) is performed with the distribution aggregate load as well as associated DER Volt-Var characteristic as explained in Section II-B using Matlab. Once the substation voltage is obtained, the LTC measures the voltage and compares that with the allowable voltages in the LTC bandwidth. A tap operation is then initiated after a predetermined time delay plus four seconds corresponding to tap mechanical movement. The new tap position alters the substation transformer turns ratio, which is used at the corresponding future time step. The entire algorithm is depicted in Fig. 5.

### E. FLICKER

A simplified approach based on IEEE Standard 1453-2015 Clause 7 [29] was used to calculate the short-term (10-minute intervals) flicker severity as

$$P_{st} = \left(\frac{d}{d_{Pst=1}}\right) * F \tag{5}$$

**TABLE 3. Eight Cases Were Established for High Penetration of PV**

| Cases | LTC Bandwidth (Volt) | Tap Operation Mode | Time Delay Mode | Time Delay (second) |
|---|---|---|---|---|
| **1** | 2 | Ignore | Definite | 15 |
| **2** | 3 | Ignore | Definite | 15 |
| **3** | 2 | Block | Definite | 15 |
| **4** | 3 | Block | Definite | 15 |
| **5** | 2 | Ignore | Definite | 45 |
| **6** | 3 | Ignore | Definite | 45 |
| **7** | 2 | Block | Definite | 45 |
| **8** | 3 | Block | Definite | 45 |

**TABLE 4. Summary of the Substation LTC Operation in Scenario 1, Cases 1 Through 16**

| Cases | # Tap Operations | Cases | # Tap Operations |
|---|---|---|---|
| 1 | 66 | 9 | 22 |
| 2 | 2 | 10 | 2 |
| 3 | 30 | 11 | 22 |
| 4 | 2 | 12 | 2 |
| 5 | 30 | 13 | 16 |
| 6 | 2 | 14 | 2 |
| 7 | 18 | 15 | 16 |
| 8 | 2 | 16 | 2 |

where $d$ is the maximum voltage variation at the analyzed interval, $d_{Pst=1}$ is the value corresponding to the 120 V lamp curve [29], and $F$ is the shape factor of the voltage variation that can be varied between 0 and 1. Here, the voltage change/minute is set to 7.5 based on our sampling time of 4 seconds since with rapid scattered cloud movement changes in nearly every two samples is observed ($\frac{60}{8} = 7.5$). According to [29] for a rate of change of 7.5 changes/minute (Fig. 5 or Table 4 in [29]), $d_{Pst=1} = 1.7$. In addition, $F$ depends on the wave shape and was set to 1. The visibility thresholds for the distribution (MV) bus and transmission (HV) substation bus flicker were considered to be 0.9 $P_{st}$ and 0.8 $P_{st}$, respectively, based on the recommended planning levels in the IEEE Std. 1453-2015.

## III. SIMULATION RESULTS

A time-series simulation was created in Matlab that calls the solar irradiation at the rate of 1 sample/4 s and uses the interpolated loads at the same frequency for load flow. A total of 12,645 data points is used that represents a time range from 6 am to around 8 pm. A solar-powered DER unit is connected at Substation CA downstream of the substation LTC as shown in Fig. 2. The transmission has lumped loads at remaining substations except Substation CA where the distribution circuit was modeled in detail comprising of three distribution feeders. The Matlab-based load flow algorithm solves the load flow that includes the reactive power provided by the DER, the LTC tap operation, and the total distribution load at Substation CA. Once the voltage is obtained by the transmission load flow, the OpenDSS simulator is called at the time step and finds the distribution feeder nodal voltages where one can assure the downstream distribution voltages are satisfactory. All the preceding steps are performed at every sampling time (every 4 seconds). Several simulation scenarios were conducted to observe the effect of the intermittent solar power on the transmission and distribution voltages as well as on the operation of the LTC in the presence of the DER Volt-Var function. Under the no-PV condition, the number of substation LTC operations in the entire day is $< 6$ operations when using an LTC bandwidth of 2 V with a time delay of 30 s.

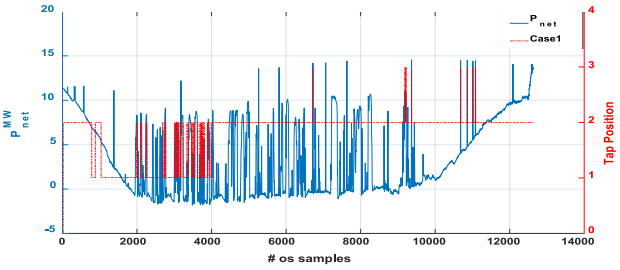


**FIGURE 6. Net Power at the Substation CA When 20 MW Solar Farm has Used the LTC Operation in Case 1.**

### A. SCENARIO 1

Here, the effects of bandwidth on the operation of substation LTC and the distribution voltage and flicker during the high and low penetration of PV are discussed. It is assumed that the DER Volt-Var control is off and the transmission capacitor banks are disconnected. All distribution capacitor banks and line voltage regulators are on. For making a comparison, ignore and block were considered as two modes of LTC operation with definite 15 and 45 seconds time delay. Eight cases were established for high penetration of PV i.e., 20 MW PV as shown in Table 3.

The aforementioned cases were repeated for low penetration of PV; i.e., 5 MW PV, in *Cases 9* through *16*.

The 0 and 12645 in the x-axis of Fig. 6 to Fig. 10 and Fig. 12 represent the 6:00 AM and 8:00 PM, respectively. Each interval between two consecutive values in the x-axis of these figures indicates 4-seconds. The net active power at the Substation CA during the penetration of 20 MW solar farm, which includes the total load power, losses, and generated power by the PV, and the substation LTC operation in *Case 1* are depicted in Fig. 6, respectively. Fig. 6 indicates that the substation LTC operates during drastic changes in the net load. While these changes can occur any time throughout the day due to cloud movement, that chance of large changes in the net load is higher in the reverse power time period due to the change in the current direction and series voltage drop. Fig. 7 compares the LTC tap operation with 2 V and 3 V bandwidths around the same 115 V tap center. Thus, increasing the bandwidth of the substation LTC can significantly decrease the number of LTC operations under highly intermittent solar

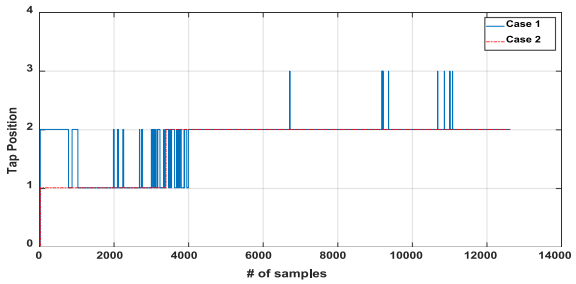


**FIGURE 7.** Effects of bandwidth on the substation LTC operation

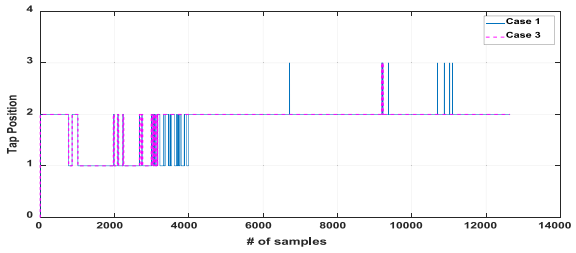


**FIGURE 8.** Effects of the substation LTC block mode (*Case_3*).

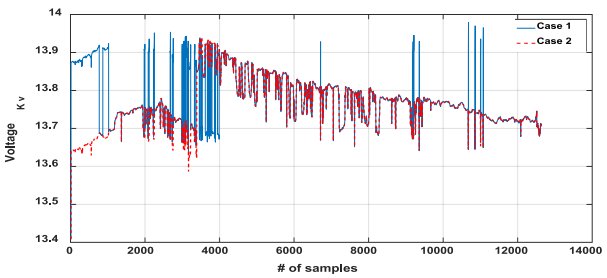


**FIGURE 9.** Distribution Bus Voltage of *Case_1* to *Case_2*.

power. Case 3 utilizes the 2 V bandwidth but applies block-mode operation and compares with results of Case 1 as shown in Fig. 8. The block mode can decrease the number of LTC operations but it cannot solve the LTC hunting action. Fig. 9 depicts the 13.8 kV distribution bus voltages in Cases 1 and 2 (see Fig. 2).

The voltage at the end of Feeders C102 and C104 are depicted in Fig. 10. The high voltage fluctuations in the figure are due to the substation LTC operations whereas the smaller ones are caused by the intermittency in the DER power generation.

Flicker levels at the distribution 13.8 kV bus and the Substation CA 115 kV transmission bus for C*ases 1 and 2* are shown in Fig. 11. Unlike at the distribution bus where a relatively high flicker amount is observed, the transmission flicker is not significant.

The net power at the Substation CA when the 5 MW solar farm is used at the distribution bus (*Case 9 through Case 16*) is depicted in Fig. 12 along with the substation LTC operation in *Case 9*.

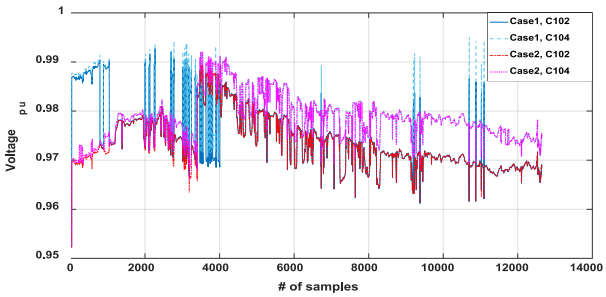


**FIGURE 10.** Voltages at the End of Feeders C102 and C104 for *Case 1* and *Case 2*.

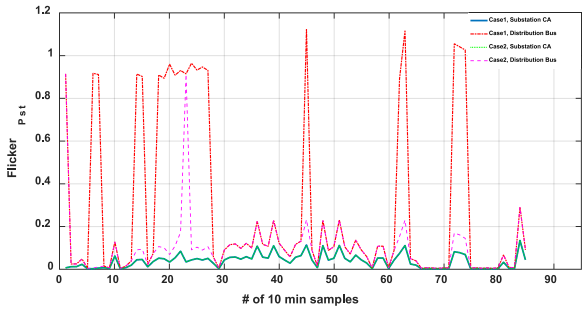


**FIGURE 11.** Flicker in the Substation CA and Distribution bus for *Case 1* and *Case 2*.

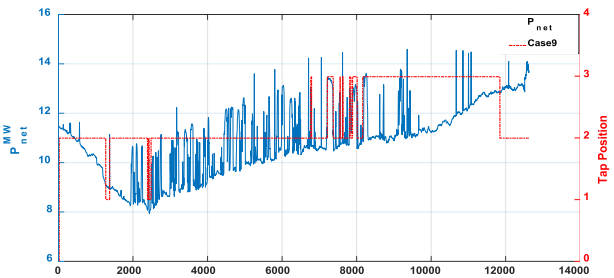


**FIGURE 12.** Net Power at the Substation CA and the LTC Operation in *Case 9*.

The summary of the substation LTC operation for all of the 16 cases is expressed in Table 4. From Table 4 the number of LTC operation decreases by increasing the bandwidth, changing the mode of operation from ignore to block, or increasing the time delay; however, increasing the bandwidth is more effective than the other options.

### *B. SCENARIO 2*

In this scenario, the effects of characteristics of DER Volt-Var control, i.e., $V_1$, $V_2$, $V_3$, and $V_4$ in Fig. 3, on the operation of LTC is investigated and 20 different cases are presented in Table 5.

The distribution voltage and flicker during high PV penetration (20 MW) with the LTC bandwidth of 2 V and time delay of 45 s are studied. Here, 2 V bandwidth with 45 s time delay are considered as base cases and are not altered.

**TABLE 5.** Scenario 2 Results Comparison—Effect of DER Volt-Var Control on LTC Tap Operations

| Cases | $V_1$(pu) min, max | $V_2$(pu) min, max | $V_3$(pu) min, max | $V_4$(pu) min, max | # Tap Op | | $V_2$-$V_1$ pu | DeadBand (Fig. 3) | Average of Q (KVAr) | |
|---|---|---|---|---|---|---|---|---|---|---|
| | | | | | Ignr | Blk | | | Ignr | Blk |
| 1-2 | 0.96<br>0.77, 1.03 | 0.99<br>0.95, 1.05 | 1.01<br>0.95, 1.05 | 1.04<br>0.97, 1.18 | 30 | 18 | 0.03 | 0.02 | 5.1 | 20.2 |
| 3-4 | 0.97,<br>0.77, 1.03 | 0.999<br>0.95, 1.05 | 1.001<br>0.95, 1.05 | 1.03<br>0.97, 1.18 | 2 | 2 | 0.029 | 0.002 | 691.8 | 691.8 |
| 5-6 | 0.975<br>0.77, 1.03 | 0.999<br>0.95, 1.05 | 1.001<br>0.95, 1.05 | 1.025<br>0.97, 1.18 | Conv failed | | 0.024 | 0.002 | Conv failed | |
| 7-8 | 0.974<br>0.77, 1.03 | 0.999<br>0.95, 1.05 | 1.001<br>0.95, 1.05 | 1.026<br>0.97, 1.18 | 2 | 2 | 0.025 | 0.002 | 782.7 | 782.7 |
| 9-10 | 0.96<br>0.77, 1.03 | 0.993<br>0.95, 1.05 | 1.007<br>0.95, 1.05 | 1.04<br>0.97, 1.18 | 12 | 4 | 0.033 | 0.014 | 41.4 | 56.3 |
| 11-12 | 0.97<br>0.77, 1.03 | 0.995<br>0.95, 1.05 | 1.008<br>0.95, 1.05 | 1.033<br>0.97, 1.18 | 8 | 2 | 0.025 | 0.013 | 187.7 | 168.4 |
| 13-14 | 0.97<br>0.77, 1.03 | 0.996<br>0.95, 1.05 | 1.02<br>0.95, 1.05 | 1.06<br>0.97, 1.18 | 6 | 2 | 0.026 | 0.024 | 267.4 | 242.4 |
| 15-16 | 0.97<br>0.77, 1.03 | 0.996<br>0.95, 1.05 | 1.01<br>0.95, 1.05 | 1.036<br>0.97, 1.18 | 6 | 2 | 0.026 | 0.014 | 267.4 | 242.5 |
| 17-18 | 0.967<br>0.77, 1.03 | 0.996<br>0.95, 1.05 | 1.01<br>0.95, 1.05 | 1.039<br>0.97, 1.18 | 8 | 2 | 0.029 | 0.014 | 246.9 | 214 |
| 19-20 | 0.972<br>0.77, 1.03 | 0.996<br>0.95, 1.05 | 1.01<br>0.95, 1.05 | 1.034<br>0.97, 1.18 | Conv failed | | 0.024 | 0.014 | Conv failed | |

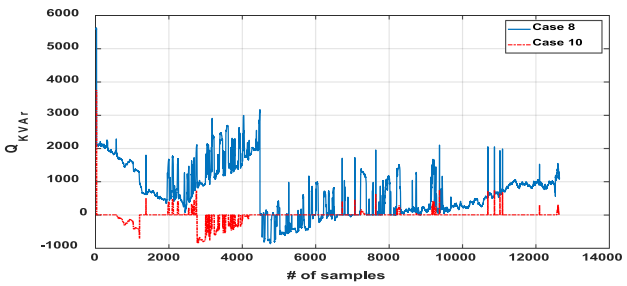


**FIGURE 13.** Injected/Absorbed Reactive Power by Volt-Var Control for Scenario 2, Cases 8 and 10.

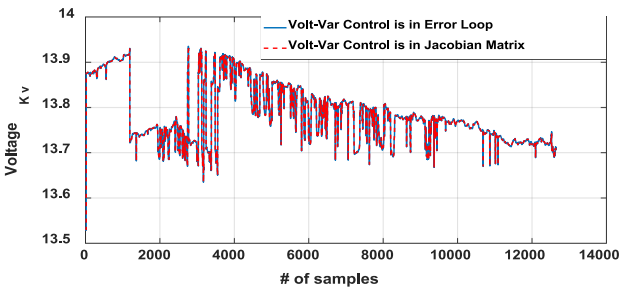


**FIGURE 14.** Distribution Bus Voltage Scenario 2, Case 9, DER Volt-Var Control in Error Loop vs. Jacobian Matrix (proposed approach).

The results of this scenario for different cases are shown in Table 5. In Table 5, the min and max underneath the characteristics show the lower and upper permissible ranges according to Table 8 of the IEEE Std 1547-2018 [15]. Each characteristic is simulated for two different LTC modes of operation; i.e., Ignore (Ignr) and Block (Blk). The number of the substation LTC operations for Ignore and Block modes are given in column 6. In column 7, $V_2 - V_1$ represents the slope/steepness of the Volt-Var curve (see Fig. 3) under constant $Q_{max}$. If the steepness of the DER Volt-Var curve is large, it can make the power grid unstable and cause the load flow program to not converge due to inappropriate reactive power injection/absorption amounts. The last column in this table represents the average injected/absorbed reactive power (in KVAr) over the entire day. The average reactive power is used as an indicator of the reactive power control cost. For instance, Fig. 13 represents the injected/absorbed reactive power in Case 8, which has the highest average of reactive power, and case 10, which has a moderate average of reactive power. From Table 5, for the steeper slope and smaller deadband the average injected/absorbed reactive power (KVAr) is higher. The distribution bus voltage in Case 9 is utilized to verify the accuracy of the result of using DER Volt-Var control in the jacobian matrix. Fig. 14 shows that the results of both approaches; i.e., when the DER Volt-Var control is in the error loop and when it is considered in the jacobian matrix, are pretty similar.

### C. SCENARIO 3

In this scenario, the effects of several low power DERs, here PV inside the distribution feeders, on the transmission and distribution networks instead of one large DER installation located upstream of the distribution feeder is discussed. For this purpose, ten 2 MW PVs are considered on Feeder C104, three at beginning of the feeder close to the substation, three at the middle of the feeder, and 4 at the end of the feeder. The substation LTC settings are set to 2 V bandwidth, 115 V bandcenter, 45 s time delay, and Ignore as the mode of operation. The results of this scenario are very similar to those

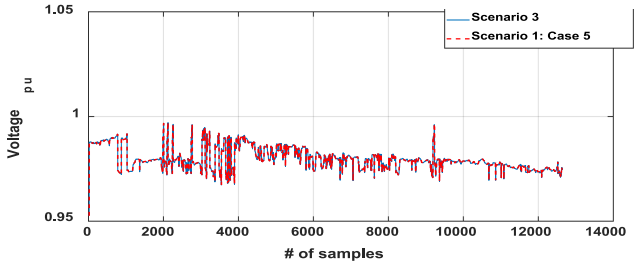


**FIGURE 15.** The voltage at the End of Feeder C104.

of *Case 5 (Scenario 1) discussed* in Section III.A as shown in Fig. 15, which shows the voltage at the end of the feeder C104 for *Scenario 3* and *Case 5* of *Scenario 1*.

## IV. CONCLUSION

This study investigates the effects of distribution-level DER units on the transmission and distribution systems including substation LTC operation, voltage fluctuation, and flicker in both transmission and distribution networks. It was shown that with the conventional LTC settings, the high penetration of DER units can cause excessive operation of the substation LTC that leads to a higher fluctuation in distribution voltage and consequently higher flicker in the distribution side. In order to mitigate the excessive LTC operations, the LTC controller mode of operation was changed from Ignore (conventionally used by industry) to Block. While the new setting reduced the number of tap operations by half, the LTC still operates more than the normal. Further reduction in tap operations is achieved by an increase in the bandwidth of the substation LTC. In addition, it was shown that the DER Volt-Var control can be employed to alleviate the hunting action in the substation LTC if the values of Volt-Var characteristics are chosen appropriately. The advantage of using the DER Volt-Var control being that the LTC bandwidth can be still retained at the conventional setting of 2 V and a reasonable time delay of 45 s can be used, which offers tighter regulation for distribution feeder voltage profiles. The proposed enhanced load flow algorithm which directly incorporates the DER Volt-Var characteristics as part of the Jacobian matrix was benchmarked with the error loop method. While both methods showed similar results, the Jacobian matrix approach was much faster in convergence during discrete changes such as substation LTC tap operations.

## REFERENCES

[1] Global Status Report -A Comprehensive Annual Overview of the State of Renewable Energy, REN21, 2019.
[2] Global Status Report -A Comprehensive Annual Overview of the State of Renewable Energy, REN21, 2018.
[3] R. A. Walling, R. Saint, R. C. Dugan, J. Burke, and L. A. Kojovic, "Summary of distributed resources impact on power delivery systems," *IEEE Trans. Power Del.*, vol. 23, no. 3, pp. 1636–1644, Jul. 2008.
[4] I. Song, W. Jung, J. Kim, S. Yun, J. Choi, and S. Ahn, "Operation schemes of smart distribution networks with distributed energy resources for loss reduction and service restoration," *IEEE Trans. Smart Grid*, vol. 4, no. 1, pp. 367–374, Mar. 2013.
[5] R. J. Campbell, "Weather-related power outages and electric system resiliency," in *Proc. Congressional Res. Service, Library Congr.*, Washington, DC, USA, 2012, Art. no. R42696.
[6] A. M. Salman, Y. Li, and M. G. Stewart, "Evaluating system reliability and targeted hardening strategies of power distribution systems subjected to hurricanes," *Rel. Eng. Syst. Safety*, vol. 144, pp. 319–333, Dec. 2015.
[7] K. A. Wheeler, M. Elsamahy, and S. O. Faried, "A novel reclosing scheme for mitigation of distributed generation effects on overcurrent protection," *IEEE Trans. Power Del.*, vol. 33, no. 2, pp. 981–991, Apr. 2018.
[8] F. Blaabjerg, Y. Yang, D. Yang, and X. Wang, "Distributed power-generation systems and protection," *Proc. IEEE*, vol. 105, no. 7, pp. 1311–1331, Jul. 2017.
[9] P. P. Barker and R. W. De Mello, "Determining the impact of distributed generation on power systems. I. Radial distribution systems," in *Proc. Power Eng. Soc. Summer Meeting*, Seattle, WA, USA, 2000, vol. 3, pp. 1645–1656.
[10] S. Eftekharnejad, V. Vittal, G. T. Heydt, B. Keel, and J. Loehr, "Impact of increased penetration of photovoltaic generation on power systems," *IEEE Trans. Power Syst.*, vol. 28, no. 2, pp. 893–901, May 2013.
[11] C. Wang, K. Yuan, P. Li, B. Jiao, and G. Song, "A projective integration method for transient stability assessment of power systems with a high penetration of distributed generation," *IEEE Trans. Smart Grid*, vol. 9, no. 1, pp. 386–395, Jan. 2018.
[12] E. Serban, M. Ordonez, and C. Pondiche, "Voltage and frequency grid support strategies beyond standards," *IEEE Trans. Power Electron.*, vol. 32, no. 1, pp. 298–309, Jan. 2017.
[13] Common Functions for Smart Inverters, Version 3. EPRI, Palo Alto, CA: 2013. 3002002233.
[14] Grid Impacts of Distributed Generation with Advanced Inverter Functions: Hosting Capacity of Large-Scale Solar Photovoltaic Using Smart Inverters. EPRI, Palo Alto, CA: 2013. 3002001246.
[15] Photovoltaics, D. G. and Storage, E., *IEEE Standard For Interconnection and Interoperability of Distributed Energy Resources With Associated Electric Power Systems Interfaces*. IEEE Stdandard, 1547-2018, 2018.
[16] T. Stetz, F. Marten, and M. Braun, "Improved low voltage grid-integration of photovoltaic systems in germany," *IEEE Trans. Sustain. Energy*, vol. 4, no. 2, pp. 534–542, Apr. 2013.
[17] A. Singh and P. W. Lehn, "Nonlinear reactive power control scheme to maximize penetration of distributed generation in distribution networks," in *Proc. IEEE Elect. Power Energy Conf.*, Saskatoon, SK, Canada, 2017, pp. 1–6.
[18] M. A. Shuvra and B. H. Chowdhury, "Autonomous control of smart inverters in grid connected and islanded mode," in *Proc. IEEE Power Energy Soc. Innovative Smart Grid Technol. Conf.*, Washington, DC, USA, 2017, pp. 1–5.
[19] X. Zhao, L. Chang, R. Shao, and K. Spence, "Power system support functions provided by smart inverters—A review," *CPSS Trans. Power Electron. Appl.*, vol. 3, no. 1, pp. 25–35, Mar. 2018.
[20] M. Kraiczy, T. Stetz, and M. Braun, "Parallel operation of transformers with on load tap changer and photovoltaic systems with reactive power control," *IEEE Trans. Smart Grid*, vol. 9, no. 6, pp. 6419–6428, Nov. 2018.
[21] T. T. Ku, C. H. Lin, C. S. Chen, and C. T. Hsu, "Coordination of transformer on-load tap changer and PV smart inverters for voltage control of distribution feeders," in *Proc. IEEE/IAS 54th Ind. Commercial Power Syst. Techn. Conf.*, Niagara Falls, ON, Canada, 2018, pp. 1–8.
[22] D. Ranamuka, A. P. Agalgaonkar, and K. M. Muttaqi, "Online voltage control in distribution systems with multiple voltage regulating devices," *IEEE Trans. Sustain. Energy*, vol. 5, no. 2, pp. 617–628, Apr. 2014.
[23] T. Aziz and N. Ketjoy, "Enhancing PV penetration in LV networks using reactive power control and on load tap changer with existing transformers," *IEEE Access*, vol. 6, pp. 2683–2691, 2018.
[24] M. Kraiczy, M. Braun, G. Wirth, T. Stetz, J. Brantl, and S. Schmidt, "Unintended interferences of local voltage control strategies of HV/MV transformer and distributed generators," in *Proc. Eur. PV Solar Energy Conf. Exhib.*, Paris, France, Oct. 2013, pp. 4217–4224.
[25] Eaton, *AUTOVAR 300 Automatically Switched Capacitor Bank*, Instruction Manual IM02607003E, Sep. 2013.
[26] T. M. Blooming and D. J. Carnovale, "Capacitor Application Issues," *IEEE Trans. Ind. Appl.*, vol. 44, no. 4, pp. 1013–1026, Jul./Aug. 2008.

[27] Waukesha, Load tap changer, UZD Technical Manual, 2016.
[28] LTC Transformer Control System Including Paralleling and Backup Control, Beckwith Application Guide.
[29] *IEEE Recommended Practice for the Analysis of Fluctuating Installations on Power Systems*, IEEE Stdandard 1453-2015, 2015.
[30] R. C. Dugan, "Reference guide: The open distribution system simulator (opendss)," Electric Power Research Institute, Inc 7, 2012.

**MOHAMMAD MEHDI REZVANI** (Student Member, IEEE) received the B.S. degree from the Isfahan University of Technology, Isfahan, Iran, in 2014, and the M.S. degree from Shahid Beheshti University, Tehran, Iran, in 2017, both in electrical engineering. He is currently working toward the Ph.D. degree in electrical engineering with Louisiana State University, Baton Rouge, LA, USA. His current research interests include distributed energy resources effects on transmission and distribution systems, steady-state and dynamic analysis of hybrid ac–dc grids, smart grid, and decentralized control.

**SHAHAB MEHRAEEN** (Member, IEEE) received the B.S. degree in electrical engineering from the Iran University of Science and Technology, Tehran, Iran, in 1995, the M.S. degree in electrical engineering from the Esfahan University of Technology, Esfahan, Iran, in 2001, and the Ph.D. degree in electrical engineering from the Missouri University of Science and Technology, Rolla, MO, USA, in 2009. Prior to his Ph.D., he worked for power generation industry for four years in power plant retrofit projects and control systems. He joined the Louisiana State University, Baton Rouge, LA, USA, in 2010. He is the Director of the Smart Grid and Renewable Power Laboratory: Control and Protection, Louisiana State University. His current research interests include micro grids, renewable energies, power systems dynamics, ac and dc protection, ac-dc grids, and smart grids. In addition, he conducts research on decentralized, adaptive, and optimal control of dynamical systems. He is a National Science Foundation CAREER awardee and holds a U.S. patent on energy harvesting and a few more pending.

**JAYANTH R. RAMAMURTHY** (Senior Member, IEEE) received the B.E. degree in electrical and electronics engineering from Osmania University, Hyderabad, India, in 2005, the M.S. degree in electrical and computer engineering from the University of Florida, Gainesville, FL, USA, in 2007, and the Ph.D. degree in electrical engineering from Michigan Technological University, Houghton, MI, USA, in 2011. He is employed as Senior Engineer, Technical Studies with Entergy Corporation since 2013. His areas of interest include power system dynamics, stability and transient modeling with applications to grid integration of renewables. He is a Registered Professional Engineer in the state of Louisiana.

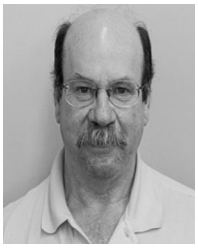

**THOMAS FIELD** (Senior Member, IEEE) received the B.S.E.E. degree from the University of New Orleans, New Orleans, LA, USA, in 1988 and the M.S.E.E. degree in power from Louisiana State University (LSU), Baton Rouge, LA, USA, in 1993. After graduating from LSU, he worked for Nashville Electric Service performing EMTP studies in the Relay and Communications group until 1998, ComEd performing real time simulator studies until 1999, Southern Company performing EMTP studies until 2004, and WAPA in the Desert Southwest transmission planning group until 2007. He is currently a Senior Staff Engineer with Entergy, New Orleans, LA, USA, where he is responsible for the real time simulator lab and university research projects. He is a member of IEEE PES, IAS, and SA. He has been a Member of several IEEE standards working groups.